

RADIO FREQUENCY SKIN DEPTH CONCEPTS IN MAGNETIC RESONANCE

RICHARD R. METT¹, JASON W. SIDABRAS, JAMES S. HYDE

Department of Biophysics, Medical College of Wisconsin,
Milwaukee, Wisconsin USA

The standard skin depth model for the penetration of electromagnetic waves into conductors is reviewed and extended to cover lossy dielectrics, such as water and polyacrylamide gel. Wavelengths and attenuation lengths for different EPR frequency bands are shown. Comparisons of finite element simulations and analytic estimates for the wavelength and attenuation length are made for four cases including: (i) field penetration into a resonant cavity wall, (ii) a plane wave in vacuum normally and (iii) obliquely incident on polyacrylamide gel, and (iv) surface coil excitation of a cylindrical sample of polyacrylamide gel. Results indicate good agreement between the analytic predictions and the first three cases, but not for the fourth. For this case, we find that the sample size must be larger than about a wavelength before the analytic wavelength estimate becomes close to the actual wavelength. Otherwise, geometrical effects dominate the phase of the penetrating fields. We also find that the attenuation length is dominated by geometrical effects even when the sample size is comparable to a wavelength.

INTRODUCTION

We have observed that the phrase “skin depth” is often used in the magnetic resonance literature in a somewhat imprecise manner. The formal definition of skin depth refers to the attenuation of a plane wave inside a conductor,

$$\delta = (\pi f \mu_0 \sigma)^{-1/2}, \quad (1)$$

where f is the frequency of oscillation, μ_0 is the magnetic permeability of free space, and σ is the conductivity. For a plane wave, the skin depth is the distance for which the amplitude of the electric or magnetic field or the current density drops by a factor of e . Since the skin depth and the conductivity are readily linked by Eq. (1), it is possible in a formal sense to use them interchangeably. However, the physical sense of the meaning of “skin depth” as a distance to which all components of the electromagnetic fields have dropped in intensity by a factor of e may no longer be valid. This paper seeks to define the areas of confusion in the context of magnetic resonance, including EPR, NMR and MRI and to provide a rigorous theoretical background.

Among the practical magnetic resonance situations where the concept of skin depth arises are the following: (i) skin depth in cavity resonators, where the electric and magnetic fields in vacuum

are out of phase and separated in space to produce a standing wave, (ii) penetration of magnetic field modulation through sidewalls of an EPR cavity, (iii) eddy currents arising from rapidly changing magnetic field gradients in a context of echo-planar imaging in MRI, where the analytical problem is similar to the field modulation problem, (iv) an aqueous sample in a microwave cavity, and (v) a surface coil that is positioned over tissue.

THEORY

The wavelength and attenuation of a wave in a isotropic linear dissipative medium, which includes conductors and lossy dielectrics, can be developed from the Maxwell equations (e.g. Ramo, Whinnery & Van Duzer, 1965). Ampere’s law and Faraday’s law can be written, respectively, as

$$\nabla \times \mathbf{H} = \mathbf{J} + \frac{\partial \mathbf{D}}{\partial t}, \quad (2)$$

$$\nabla \times \mathbf{E} = -\frac{\partial \mathbf{B}}{\partial t}, \quad (3)$$

where the usual variable definitions apply. Assuming time harmonic fields, $e^{-i\omega t}$, the constitutive relations $\mathbf{B} = \mu_0 \mathbf{H}$ and $\mathbf{D} = \epsilon \mathbf{E}$, and Ohm’s law, $\mathbf{J} = \sigma \mathbf{E}$, we can combine Eqs. (2) and (3) to form

¹ Also at: Milwaukee School of Engineering, Milwaukee, Wisconsin USA 53202-3109

$$\nabla \times \nabla \times \mathbf{E} = \frac{\omega^2}{c^2} \left(\epsilon_r + i \frac{\sigma}{\omega \epsilon_0} \right) \mathbf{E}, \quad (4)$$

where $c = (\epsilon_0 \mu_0)^{-1/2}$ represents the speed of light in vacuum and $\epsilon_r = \epsilon/\epsilon_0$ is the relative dielectric constant of the medium. On the right side of Eq. (4), there is competition between the displacement plus polarization currents, given by the term containing ϵ_r , and the conduction current, given by the term containing σ . The magnetic fields are governed by an equation of the same form as Eq. (4). The wave is thus electromagnetic. If we further assume a transverse plane wave type propagation,

$$\mathbf{E} = \mathbf{E}_0 e^{i\mathbf{k} \cdot \mathbf{r}}, \quad (5)$$

Eq. (4) gives an expression for the wavenumber,

$$k = k_0 \left(\epsilon_r + i \frac{\sigma}{\omega \epsilon_0} \right)^{1/2}, \quad (6)$$

where the free space wavenumber $k_0 = \omega/c$ is related to the free space wavelength $\lambda_0 = 2\pi/k_0$.

In a good conductor, we may neglect the polarization plus displacement currents compared to the conduction current $\epsilon_r \ll \sigma/\omega \epsilon_0$ and find

$$k = k_0 \left(i \frac{\sigma}{\omega \epsilon_0} \right)^{1/2} = \frac{(1+i)}{\delta}, \quad (7)$$

where the standard skin depth is given by Eq. (1). There, $\omega = 2\pi f$. We see that for propagation of the wave through a conductor along z ,

$$\mathbf{E} = \mathbf{E}_0 e^{ikz} = \mathbf{E}_0 e^{i(1+i)z/\delta} = \mathbf{E}_0 e^{iz/\delta} e^{-z/\delta}, \quad (8)$$

Table 1 Attenuation length and wavelength of various linear materials.

	free space	graphite AF-5		silver		water		30% poly-acrylamide gel	
$f(\text{MHz})$	$\lambda(\text{cm})$	$\delta_a(\mu\text{m})$	$\lambda(\mu\text{m})$	$\delta_a(\mu\text{m})$	$\lambda(\mu\text{m})$	$\delta_a(\text{cm})$	$\lambda(\text{cm})$	$\delta_a(\text{cm})$	$\lambda(\text{cm})$
0.1	300,000	6,600	42,000	200	1,300	27,000	33,000		
600	50	85	540	2.6	16	110	5.7		
1,200	25	60	380	1.8	12	16	2.8	2.0	3.4
3,200	9.4	37	230	1.1	7.1	2.1	1.1		
9,500	3.2	21	130	0.65	4.1	0.28	0.39		
35,000	0.86	11	70	0.34	2.1	0.049	0.15		
94,000	0.32	6.9	43	0.21	1.3	0.025	0.088		

Table 2. Conductivities and dielectric constants for the linear materials of Table 1.

	free space	graphite AF-5 ^a	silver ^b	water	30% poly-acrylamide gel
$f(\text{MHz})$	ϵ_r	$\sigma(\Omega^{-1}\text{m}^{-1})$	$\sigma(\Omega^{-1}\text{m}^{-1})$	ϵ_r	ϵ_r
0.1				$78.2 + i 31.3^b$	
600				$77.5 + i 1.24^c$	
1,200				$77.0 + i 4.24^c$	$49.5 + i 28.5^d$
3,200	1	5.79×10^4	6.22×10^7	$76.7 + i 12.6^c$	
9,500				$63.0 + i 29.0^c$	
35,000				$23.0 + i 31.1^c$	
94,000				$9.00 + i 14.5^c$	

^afrom Sheppard, Mathes & Bray (1987).

^bfrom Ramo, Whinnery & Van Duzer (1965).

^cfrom Weil, Bolton & Wertz (1994).

^dfrom Andreuccetti, Bini, Ignesti, Olmi, Rubino & Vanni (1988).

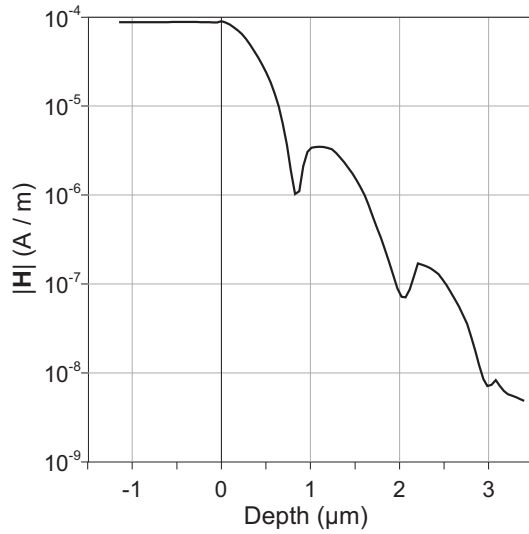


Fig. 1. Finite element simulation of the rf magnetic field penetration into a silver cylindrical TE_{01U} uniform field mode cavity wall. The cavity radius was 5.65 mm and the frequency was 35 GHz. A 0.1° cavity sector was used, with the metallic wall taking up a surface of dimensions $10 \mu\text{m} \times 10 \mu\text{m}$ and a depth of ten skin depths, $3.4 \mu\text{m}$. The conductivity of silver was taken as $6.17 \times 10^7 (\Omega\text{m})^{-1}$.

and the electric field attenuates by $1/e$ in a distance equal to the skin depth. At the same time, the wave has a wavelength given by

$$\lambda = 2\pi\delta. \quad (9)$$

When we think of skin depth in a conductor, the attenuation length is readily understood, but the wavelength of the field oscillation is not. Such an oscillation is shown in Fig. 1, from a finite element simulation of an electromagnetic wave as it penetrates the conducting wall of the center section of a

TE_{01U} cavity (Hyde, Mett & Anderson, 2002). The simulation is for a cavity mode at 35 GHz. The cavity is represented by the region $z < 0$ and the silver conducting wall by $z > 0$. The magnetic field magnitude simultaneously oscillates and decays in the region $z > 0$, following Eq. (8). The skin depth for this case is $0.34 \mu\text{m}$ and matches the average attenuation shown in Fig. 1. The distance between the dips in the magnetic field magnitude represent the half-wavelength of the electromagnetic wave. A full wavelength of $2.1 \mu\text{m} \approx 2\pi\delta$ is visible.

In a lossy medium, the dielectric constant is often given real and imaginary parts (Von Hippel, 1954),

$$\epsilon_r = \epsilon_{rr} + i\epsilon_{ri} = \epsilon_{rr}(1 + i \tan \zeta), \quad (10)$$

where $\tan \zeta$ is the loss tangent. In comparing Eq. (10) with Eq. (6), there is an equivalence of the conductivity (which is real) and the imaginary part of the dielectric constant. The conductivity equivalent of an imaginary part of the dielectric constant is

$$\sigma = \omega\epsilon_0\epsilon_{ri} = \omega\epsilon_0\epsilon_{rr} \tan \zeta, \quad (11)$$

whereas the imaginary dielectric constant equivalent of a conductivity is

$$\epsilon_{ri} = \frac{\sigma}{\omega\epsilon_0}. \quad (12)$$

However, one may not write an equivalent skin depth as such because the real and imaginary parts of the wavenumber have different proportions, unlike Eq. (7). Substituting Eq. (10) into Eq. (6) and taking $\sigma = 0$, we find

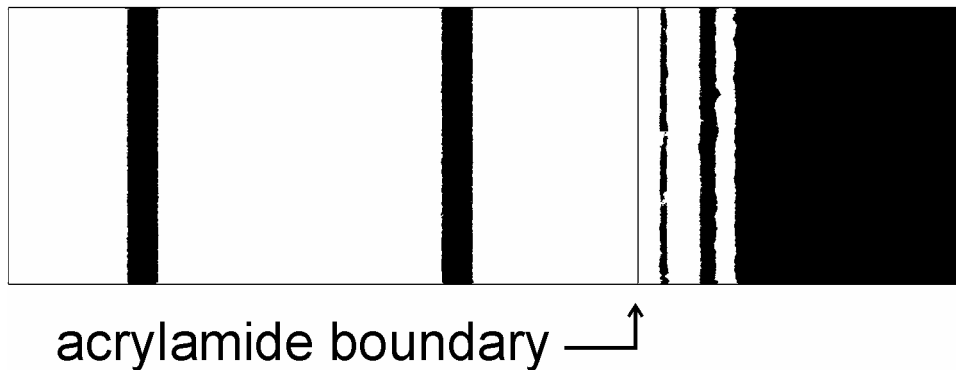


Fig. 2. Finite element simulation of a plane wave in vacuum incident normally on a slab of 30% polyacrylamide gel. Electric field magnitude in space is shown with white maximum and black minimum. The plane wave propagates from left to right and has a frequency of 1.2 GHz. The horizontal dimension of the polyacrylamide gel is 1.3 cm. The wavelength and attenuation length in the gel match the entries in Table 1.

$$k = k_0 \sqrt{\epsilon_{rr}} (1 + i \tan \zeta)^{1/2}. \quad (13)$$

The electric field in the lossy medium now can be written

$$\mathbf{E} = \mathbf{E}_0 e^{ikz} = \mathbf{E}_0 e^{ik_r z} e^{-k_i z}, \quad (14)$$

which shows that the wavelength in the lossy medium is given by

$$\lambda = \frac{2\pi}{k_r} = \frac{\lambda_0}{\sqrt{\epsilon_{rr}} \operatorname{Re}[(1 + i \tan \zeta)^{1/2}]}, \quad (15)$$

and the attenuation length by

$$\delta_a = \frac{1}{k_i} = \frac{\lambda_0}{2\pi \sqrt{\epsilon_{rr}} \operatorname{Im}[(1 + i \tan \zeta)^{1/2}]}. \quad (16)$$

The attenuation length given by Eq. (16) may be considered an equivalent skin depth, but the wavelength given by Eq. (15) is not $2\pi\delta_a$.

RESULTS

The wavelength and attenuation length in different lossy media at various EPR operating frequencies have been calculated using Eqs. (15) and (16).

Results are shown in Table 1 below. Conductivities and dielectric constants used to produce Table 1 are given in Table 2.

The skin depth model applies when the perpendicular field scale length or material surface geometrical scale length $a \gg \delta$. The skin depth is the attenuation length of the current or field penetration into the conductor, but predicts nothing about the effect of those surface currents on the total surrounding field strength. Thus, any surface current, including, but not limited to an eddy current, will have a skin depth. Time-varying currents in a conductor produce time-varying magnetic fields and these fields induce “eddy currents” in nearby conductors. Eddy currents can be produced by rapidly switching currents in gradient coils used in MRI and also by currents in magnetic field modulation coils in EPR. When the time-changing magnetic fields are perpendicular to the surface of a conductor, the eddy currents reduce the magnetic fields from what they would be in the absence of the conductor and can also result in phase shifts. When the time-changing magnetic fields are parallel to the surface, the eddy currents increase the field strength. Only eddy magnetic field components parallel to the static field contribute deleterious effects in magnetic resonance. This reduces the number of design constraints.

In order to address questions of penetration and skin depth in conducting samples, finite element simulations were carried out using Ansoft High



Fig. 3. Finite element simulation of a plane wave in vacuum with grazing incidence on a slab of 30% polyacrylamide gel. Electric field magnitude in space is shown with white maximum and black minimum. The plane wave propagates from left to right and has a frequency of 1.2 GHz. The horizontal dimension of the polyacrylamide gel is 1.3 cm. The wavelength of the plane wave in vacuum decreases as it nears the gel interface and the wave enters the gel at an angle approaching 90° , as shown. The wavelength and attenuation length in the gel are the same as for normal incidence (Fig. 2) and again match the entries in Table 1.

Frequency Structure Simulator, version 9.2 (Ansoft Corp., Pittsburgh, PA) on a dual processor Compaq W8000 workstation, with two Intel Xeon 1.7 GHz Pentium processors and 4 GB of RAM.

Figure 2 shows results of a finite element simulation of the electric field magnitude of a 1.2 GHz plane wave in vacuum normally incident on a slab of 30% polyacrylamide gel. This material has dielectric properties that are equivalent to biological tissue (Andreuccetti, Bini, Ignesti, Olmi, Rubino & Vanni, 1988). The wavelength and attenuation length are seen to match those given in Table 1. Figure 3 shows the electric field magnitude of a plane wave obliquely incident on a slab of 30% polyacrylamide gel. Here, the rf electric field of the incident plane wave is nearly perpendicular to the interface, while the rf magnetic field is tangential. Note that the vacuum wavelength shortens near the interface and, once entering the gel, the wave propagates in a direction nearly perpendicular to the interface. The wave in the gel is a plane wave, nearly identical to that of Fig. 2, and the wavelength and attenuation length again match those given in Table 1.

Figure 4 shows the axial magnetic field phase (a) and magnitude (b) generated by a circular loop of wire near a cylinder of polyacrylamide gel. The loop is driven by a unit current at 1.2 GHz and has a diameter of 1.0 cm. The geometry is similar to that considered by Salikhov, Hirata, Walczak, and Swartz (2003). The axes of the loop and sample cylinder coincide and the loop location is 0.4 mm above the vacuum-gel interface. The ratio of di-

ameter to length of the sample is unity. A decrease of wavelength with sample size is evident from Fig. 4(a). For the 10 mm sample, much smaller than the wavelength of 34 mm (Table 1), the phase variation of the axial magnetic field through the sample is significantly less than that predicted by the plane wave model, 360° in one wavelength. However, for the 40 mm sample the phase goes through 180° in approximately one-half wavelength. Evidently, when an object has a linear dimension equal to a wavelength or larger, the wavelength in the material approaches the wavelength predicted by the plane wave model.

The corresponding magnitude dependence of the axial magnetic field attenuation as a function of sample size is shown in Fig. 4(b). A more complex dependency on the sample size is evident. The non-monotonic behavior is caused by wave propagation in directions other than axial and by reflections from the interfaces. Strictly speaking, the plane wave model applies to transverse electric and magnetic fields, which, for axial propagation, have field components perpendicular to the axial magnetic field plotted in Fig. 4(b). Larger samples are likely required to show the attenuation lengths predicted by Table 1. Due to geometry, the attenuation lengths apparent from Fig. 4(b) are several times smaller than the 2.0 cm value predicted by the plane wave model.

Generally, a relatively small surface coil placed on a larger region of tissue results in the effects found in Fig. 4. For a cavity into which a sample has been inserted, this is not the case. In rectangu-

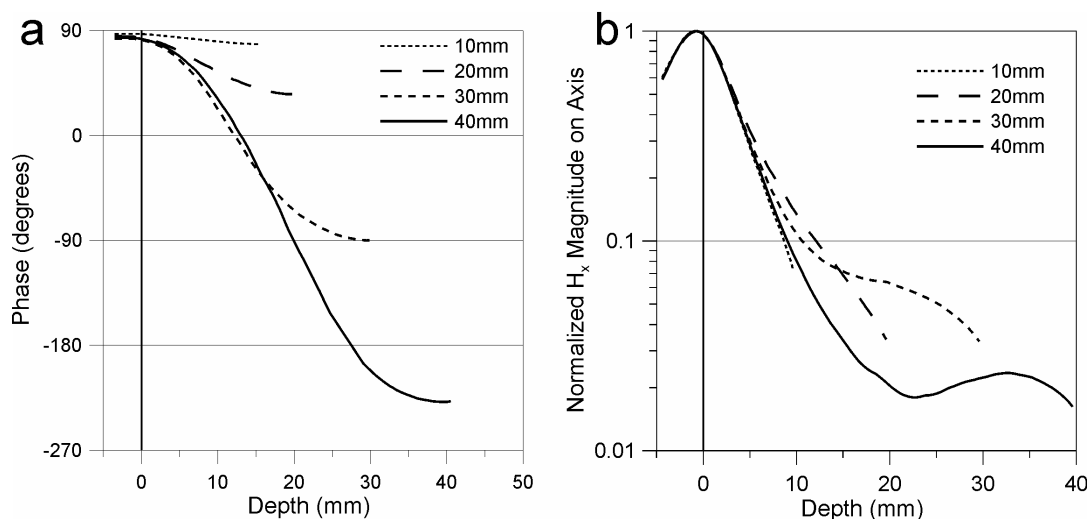


Fig. 4. Finite element simulations of the a) phase and b) magnitude of the axial magnetic field produced by a 1.0 cm diameter loop of 0.8 mm diameter wire driven at 1.2 GHz and situated near a sample cylinder of 30% polyacrylamide gel. The field is plotted as a function of axial position with $x = 0$ as the location of the sample surface and $x = -0.4$ mm as the location of the loop. The loop axis coincides with the sample cylinder axis. In each case, the sample cylinder has a ratio of diameter to length of unity. The four cases correspond to four progressively larger sample sizes with diameters of 10, 20, 30, and 40 mm.

lar geometry, the wavenumber k inside the sample is related to its dielectric properties and the frequency by the dispersion relation (see, e.g., Hyde & Mett, 2002; Mett & Hyde, 2003; Sidabras, Mett & Hyde, 2005),

$$\frac{\epsilon_r \omega^2}{c^2} = k_x^2 + k_y^2 + k_z^2 \quad (18)$$

which is equivalent to making the replacement $k \rightarrow \sqrt{k_x^2 + k_y^2 + k_z^2}$ in Eq. (13). There are also constraints that relate the wavenumbers across the material interfaces. If two of the wavenumbers are zero (no field variation in these directions), the third wavenumber obeys Eq. (13) and the attenuation length and wavelength discussion of the Theory section applies. The total variation of the fields across the different directions within the sample adjust to the constraint of Eq. (18). The wavenumbers are complex when the relative dielectric constant is complex. In some cases, one or more of the wavenumbers may be predominantly imaginary, which implies an evanescent field variation in that direction. In the other directions, this produces a more rapid field variation than predicted by the Theory section. In other geometries, e.g. cylindrical, dispersion relations similar to Eq. (18) apply.

CONCLUSIONS

We have examined skin depth in conductors and have extended the standard theory to cover lossy dielectrics, such as water and polyacrylamide gel. In a conductor, the fields simultaneously oscillate and decay with an attenuation length equal to the skin depth δ and a wavelength given by $2\pi\delta$. When the polarization and displacement currents become comparable to or greater than the conduction currents, as they are for most lossy dielectrics, the fields still simultaneously oscillate and decay, but the relationship between the attenuation length and wavelength is more complex than for a conductor, as shown by Eqs. (15) and (16). Wavelengths and attenuation lengths for different materials and EPR frequency bands are given in Table 1. A comparison of finite element simulations and the analytic estimates for the wavelength and attenuation length was made for four cases including: (i) field penetration into a resonant cavity wall, (ii) a plane wave in vacuum normally and (iii) obliquely incident on polyacrylamide gel, and (iv) surface coil excitation of a cylindrical sample of polyacrylamide gel.

Results indicate good agreement between the analytic predictions and the first three cases, but not for the fourth. For this case, the geometrical effects of boundaries cause the observed attenuation lengths and wavelengths to differ from the analytic predictions. The phase variation becomes close to 180° in one half wavelength when the sample is comparable in size to a wavelength.

Acknowledgments

This work was supported by grants EB001417 and EB001980 from the National Institute of Biomedical Imaging and Bioengineering of the National Institutes of Health.

REFERENCES

- Andreuccetti, D., Bini, M., Ignesti, A., Olmi, R., Rubino, N. & Vanni, R. (1988). Use of Polyacrylamide as a Tissue-Equivalent Material in the Microwave Range, *IEEE Trans. Biomed. Eng.* 35, 275.
- Hyde, J. S. & Mett, R. R. (2002). Aqueous sample considerations in uniform field resonators for electron paramagnetic resonance spectroscopy, *Current Topics in Biophysics* 26, 7-14.
- Hyde, J. S., Mett, R. R. & Anderson, J. R. (2002). Cavities with Axially Uniform Fields for Use in Electron Paramagnetic Resonance. III. Re-entrant Geometries. *Rev. Sci. Instrum.* 73, 4003-4009.
- Jackson, J. D. (1975). *Classical Electrodynamics*. Wiley: NY.
- Mett, R. R. & Hyde, J. S. (2003). Aqueous flat cells perpendicular to the electric field for use in electron paramagnetic resonance spectroscopy. *J. Magn. Reson.* 165, 137-52.
- Ramo, S., Whinnery, J.R. & Van Duzer, T. (1965). *Fields and Waves in Communication Electronics*, Wiley, NY.
- Salikhov, I., Hirata, H., Walczak, T. & Swartz, H. (2003). An Improved External Loop Resonator for In-Vivo L-Band EPR Spectroscopy, *J. Magn. Reson.* 164, 54-59.
- Sheppard, R. G., Mathes, D. M., Bray, D. J. eds., (1987). *Poco Graphite Inc. Properties and Characteristics of Graphite for the Semiconductor Industry*, Poco Graphite, Inc., Decatur, TX.
- Sidabras, J. W., Mett, R. R. & Hyde, J. S. (2005). Aqueous flat cells perpendicular to the electric field for use in electron paramagnetic resonance spectroscopy II. Design. *J. Magn. Reson.*, 172, 333-341.
- Von Hippel, A. (1954). *Dielectric Materials and Applications*, Artech House, Boston.
- Weil, J. A., Bolton, J. R. & Wertz, J. E. (1994). *Electron Paramagnetic Resonance*. Wiley: NY.